NANO LETTERS

pubs.acs.org/NanoLett

Glycerol-Bonded 3C-SiC Nanocrystal Solid Films Exhibiting Broad and Stable Violet to Blue-Green Emission

J. Wang,[†] S. J. Xiong,[†] X. L. Wu,*[,†] T. H. Li,[†,‡] and Paul K. Chu*[,§]

[†]National Laboratory of Solid State Microstructures and Department of Physics, Nanjing University, Nanjing 210093, People's Republic of China, [‡]College of Electronic Engineering, Guangxi Normal University, Guilin 541004, People's Republic of China, and [§]Department of Physics and Materials Science, City University of Hong Kong, Tat Chee Avenue, Kowloon, Hong Kong, China

ABSTRACT We have produced glycerol-bonded 3C-SiC nanocrystal (NC) films, which when excited by photons of different wavelengths, produce strong and tunable violet to blue-green (360−540 nm) emission as a result of the quantum confinement effects rendered by the 3C-SiC NCs. The emission is so intense that the emission spots are visible to the naked eyes. The light emission is very stable and even after storing in air for more than six months, no intensity degradation can be observed. X-ray photoelectron spectroscopy and absorption fine structure measurements indicate that the Si-terminated NC surfaces are completely bonded to glycerol molecules. Calculations of geometry optimization and electron structures based on the density functional theory for 3C-SiC NCs with attached glycerol molecules show that these molecules are bonded on the NCs causing strong surface structural change, while the isolated levels in the conduction band of the bare 3C-SiC NCs are replaced with quasi-continuous bands that provide continuous tunability of the emitted light by changing the frequencies of exciting laser. As an application, we demonstrate the potential of using 3C-SiC NCs to fabricate full-color emitting solid films by incorporating porous silicon.

KEYWORDS 3C-SiC nanocrystals, glycerol, solid films, photoluminescence

In addition to the light weight, high strength, extreme hardness, wear and corrosion resistance, and inertness, silicon carbide (SiC) nanostructures have recently attracted further interest because of their novel morphologies,[1−6] quantum-confined blue photoluminescence (PL) in solvents,[7,8] and applications in biophysics such as fluorescent biological labels.[9,10] In these applications, the surface physical and chemical properties directly determine the growth of the nanocrystals (NCs), stability in a solvent, and luminescence properties.[11] Since SiC consists of carbon or silicon outermost layers, they exhibit interesting and complicated surface structures in different surroundings. Some theoretical studies on the surface characteristics of polytypic SiC exposed to water, acetic acid, and methanol have indicated that the band gap has a strong dependence on the NC size and surface bonding structure.[4,12−16] This provides the opportunity to design suitable surface structures for practical applications by terminating the surface dangling bonds with different atoms.[17] A typical example is surface patterning on the molecular level and then using these patterns to control adsorption of proteins while maintaining their activity.[12,18−20] More recently, surface modification of SiC by organic and inorganic molecules have led to the formation of some functionalized SiC materials.[21−25] These works not only enhance our understanding of some unpredictable behavior that often takes place during processing of SiC materials but also promote applications of SiC nanostructured materials in many technique-related fields.

Luminescence from a solid film has important applications in optoelectronic devices, especially in display technology. Since the observation of tunable blue emission in some suspensions of 3C-SiC NCs,[7,8] much research has been conducted on nanostructured solid 3C-SiC materials.[11] Unfortunately, 3C-SiC solid films cannot emit tunable blue light due to the amorphous fraction of the NCs and complicated surface chemical disorder induced by oxidization.[26−33] This result indicates that effective passivation of the surface of nanostructured 3C-SiC in the form of a solid film to accomplish quantum-confined PL is a difficult problem and not well understood. This has thus hampered the use of 3C-SiC nanostructure films in modern optoelectronic devices.

Ethylene glycol, propylene glycol, glycerol, and similar compounds have a molecular structure that contains −OH groups with strong electronegativity. They can easily bond to the modified surfaces of 3C-SiC NCs leading to for instance, effective surface passivation.[34] As a result, it is possible to obtain stable tunable PL from 3C-SiC NC films. In this article, we report the broad emission properties of 3C-SiC NC films after surface modification with glycerol. We first demonstrate experimentally that the glycerol-passivated 3C-SiC NC solid films can produce strong tunable violet to

* To whom correspondence should be addressed. (X.L.W) E-mail: hkxlwu@nju.edu.cn. Fax: 86-25-83595535. Tel: 86-25-83686303. E-mail: (P.K.C) paul.chu@cityu.edu.hk.

Received for review: 02/03/2010
Published on Web: 03/08/2010

DOI: 10.1021/nl100407d | *Nano Lett.* **2010,** *10,* 1466–1471

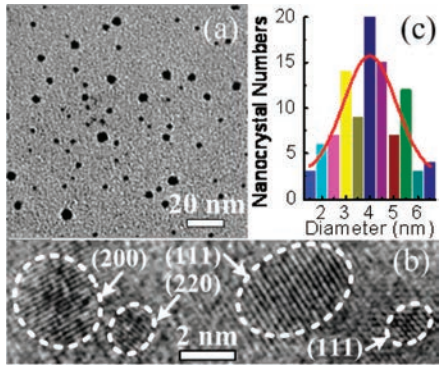

FIGURE 1. (a) A TEM image of the fabricated 3C-SiC NCs. (b) A typical high-resolution TEM image. (c) The NC number distribution with the most probable size of 4.0 nm obtained by Gaussian fitting.

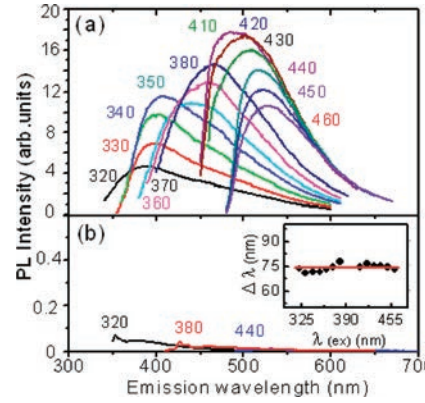

FIGURE 2. (a) PL spectra of the 3C-SiC NCs/glycerol solid film on a silicon wafer excited by different wavelengths. (b) PL spectra of pure glycerol excited by three different wavelengths. The inset in (b) shows the increment $\Delta\lambda$ between the emission and excitation wavelengths vs excitation wavelength.

blue-green PL (visible to the naked eyes) due to quantum confinement in the 3C-SiC NCs. We next reveal experimentally that the quantum-confined PL stems from a monolayer of glycerol molecules on the 3C-SiC NC surface and that glycerol bonding removes various nonradiative defects/surface states. To complement our experimental findings, we carry out theoretical calculations of the geometry optimization and electron structures for 3C-SiC NCs with attached glycerol molecules based on the density functional theory. The results show that bonding of glycerol molecules causes strong surface modification giving rise to a quasi-continuous band in the conduction band which replaces isolated levels in the case of bare NCs and provides continuously tunable emission wavelengths. As an application, we demonstrate that by coating the glycerol-passivated 3C-SiC NCs onto porous silicon (PS), 3C-SiC NCs/PS composite solid films producing strong full-color tunable PL in the whole visible range from 360 to 760 nm when the excitation wavelength changes can be fabricated. The results and discovery are relevant to modern optoelectronic devices, especially full-color displays.

The preparation of the 3C-SiC NCs has been described previously.[35] To produce the glycerol-passivated 3C-SiC films, 10 mL of a water suspension of the 3C-SiC NCs with diameters ranging from 1.5 to 6.5 nm (most probable size of ~4.0 nm) was added to a 10 mL aqueous solution with a drop of glycerol, followed by ultrasonic vibration and drying to a volume of 15 mL. Afterward, a piece of silicon substrate was put into the container until all the water vaporized leaving a thin layer on the substrate. The details regarding the transmission electron microscope (TEM) observations, PL, X-ray diffraction (XRD), X-ray photoelectron spectroscopy (XPS) and Si $L_{3,2}$-, and O *K*-edge X-ray absorption near-edge structure (XANES) measurements are similar to those reported previously.[34,35]

Figure 1a displays the TEM image of the NC distribution taken at an accelerating voltage of 200 kV, showing that the 3C-SiC NCs are nearly spherical with diameters ranging from 1.5 to 6.5 nm. No NCs with sizes larger than 6.5 nm can be observed. Figure 1b depicts the high-resolution TEM image of several representative NCs. The NCs are highly crystalline with the lattice fringes corresponding to the {111}, {200}, and {220} planes of 3C-SiC. Figure 1c shows the histogram of the NC size distribution. The NCs present an almost asymptotic centric distribution and the diameters of most of the NCs are between 3.0 and 5.5 nm. A Gaussian fit suggests that the most probable size of the NC diameters is about 4.0 nm and such NCs can exhibit distinct quantum confinement effects.[7,35] These results have also been confirmed by our XRD and Raman scattering measurements (Supporting Information Figure SI-1).

Figure 2a shows the PL spectra acquired from a solid film composed of the 3C-SiC NCs separated by glycerol coated on a silicon wafer. They are taken under excitation by various wavelengths from 320 to 460 nm emitted from a Xe lamp. The PL intensity is so high that the emission spots can be easily observed visually. As the excitation wavelength increases from 320 to 460 nm, the PL peak position increases monotonically from 380 to 540 nm. The inset in Figure 2b shows the increment $\Delta\lambda$ between the emission and excitation wavelengths versus excitation wavelengths. The flat curve indicates that the relaxed energy of the excited electrons is fixed and the results are consistent with our theoretical derivation to be discussed later. No obvious red shift in the peak can be observed at excitation wavelengths beyond 480 nm and the intensity of the PL spectrum decreases rapidly thereafter. Since the band gap of bulk 3C-SiC is 2.24 eV (554 nm), the NCs cannot be excited and PL cannot be observed.

The intensity of the PL peak centered at about 480 nm reaches a maximum at an excitation wavelength of 410 nm. Because the radii of most NCs are smaller than the Bohr radius of 3C-SiC (about 2.7 nm), the PL red shift with increasing excitation wavelength can be attributed to the quantum confinement effect in 3C-SiC NCs.[7,36,37] When the excitation wavelength is varied from 320 to 410 nm, the 3C-SiC NCs with the probable sizes can always be excited.

DOI: 10.1021/nl100407d | *Nano Lett.* **2010,** *10,* 1466–1471

Consequently, the PL intensity in this range increases with excitation wavelength. When the excitation wavelength exceeds 410 nm, the number of 3C-SiC NCs that can be excited diminishes thereby leading to a continuous decrease in the PL intensity. When the excitation wavelength is higher than 480 nm, only a few NCs can be excited and the PL intensity is weak. According to the most probable NC diameter, we can estimate the most intense emission wavelength in the PL spectrum using the following relationship:[37,38] $E^* = E_g + h^2/8\mu r^2 - 1.8e^2/4\pi\varepsilon_0\varepsilon r$, in which $E_g = 2.24$ eV is the band gap of bulk 3C-SiC, μ is the reduced mass of the exciton (electron and hole), ε is the high-frequency dielectric constant of 3C-SiC, and r is the radius of the particle. The largest PL intensity is derived to be ~478 nm, which is in good agreement with the observed value. The above analysis suggests that the NC size has an important influence on the PL energy and intensity. To rule out the possibility that the tunable PL originates from glycerol, we present in Figure 2b three typical PL spectra of pure glycerol excited by three different wavelengths. All the spectra with a small water Raman peak have very low intensities and it clearly indicates that the strong tunable PL from the solid film stems from quantum confinement rendered by the 3C-SiC NCs.

The stability of the films is investigated by storing in air for more than six months and no PL degradation and peak position shift can be observed indicating that the structure and luminescent properties of the solid film have not altered. The stability is closely related to good dispersion and effective surface passivation of the 3C-SiC NCs by glycerol molecules in the films. Three −OH groups in the glycerol molecule have strong electronegativity (Supporting Information Figure SI-2a). They can easily bond to the modified surfaces of the 3C-SiC NCs (Supporting Information Figure SI-2b) leading to effective removal of the surface/defect states. As a result, stable quantum-confined PL can be achieved from the 3C-SiC solid film.

To confirm the presence of bonding with glycerol molecules on the surface of the 3C-SiC NCs and simultaneously investigate the surface structures, we examine the C 1s, Si 2p, and O 1s core level XPS spectra of the glycerol-absorbed 3C-SiC NC films produced on a silver thin film substrate and present the corresponding results in Figure 3a. For comparison, the XPS spectra of the 3C-SiC NCs from an aqueous solution without glycerol are also shown in Figure 3b.[34] Similar to the situation in Figure 3b, these spectra in Figure 3a do not reveal the presence of bonding with water molecules due to careful evaporation and removal of the surface layer from the sample prior to the analysis. In the C 1s spectrum, the strongest peak at 283.1 eV corresponds to the SiC component.[21,39] The two shoulders on the high-energy side at 284.6 and 286.4 eV can be attributed to CH_n and $O-CH_3$,[22] respectively. Their intensities increase in comparison with those in Figures 3b1. The strong shoulder (denoted as CS) on the low-energy side at 280.8 eV, which is absent in Figure 3b1, is related to alkoxide.[40] The C 1s

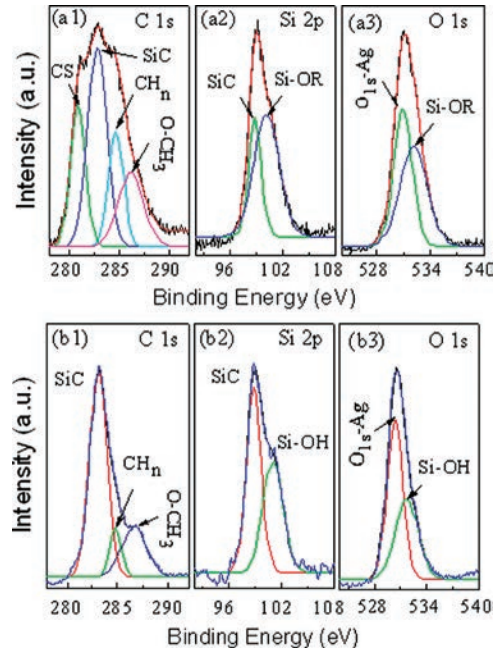

FIGURE 3. C 1s, Si 2p, and O 1s core level XPS spectra acquired from the glycerol (a1−a3) and water (b1−b3) suspension films deposited on silver film substrates. The 530.6 eV peak in the O 1s spectrum is related to the Ag substrate (ref 35).

spectrum reveals bonding of glycerol on the NC surface. In the Si 2p spectrum, the low-energy peak corresponds to the SiC component. The peak at 100.2 eV can be ascribed to the Si^{1+} state (a Si atom bonding to one oxygen atom),[34,41,42] but it is broader and has slightly lower energy than the corresponding peak at 100.7 eV in Figure 3b2. Thus, this peak is associated with the chemical bonding of Si−OR in which R is dehydrogenated glycerol component. The 531.9 eV peak in the O 1s spectrum is also broader and has a larger intensity compared to that in Figure 3b3, indicating that hydrogen in the surface Si−OH bonding has been replaced by R component.[43,44] These XPS results indicate that the Si-terminated NC surfaces are hydrophilic and connected to −OR, whereas the C-terminated surfaces are almost hydrophobic. After integration and correction for the carbon and oxygen contents using a reference sample (a clean silver surface), the Si/O atomic ratio is obtained to be 1:0.17. Using a shell approximation,[45,46] we can obtain the glycerol molecule number of 80 on each NC surface. The molecule number is about 50% more than that expected for a close-packed monolayer of glycerol ligands surrounding the NC, indicating that the Si-terminated surface has been bonded completely to glycerol molecules. X-ray absorption fine structure is an effective technique to study the near-neighbor local structure in complex materials.[34] Therefore, we have also acquired the Si $L_{3,2}$-, and O K-edge XANES spectra from the glycerol-absorbed NC film (Supposting Information Figure SI-3). The results demonstrate that glycerol molecules have bonded to the Si-terminated 3C-SiC NC surfaces, as is consistent with the XPS results. These results show that the

DOI: 10.1021/nl100407d | *Nano Lett.* **2010,** *10,* 1466–1471

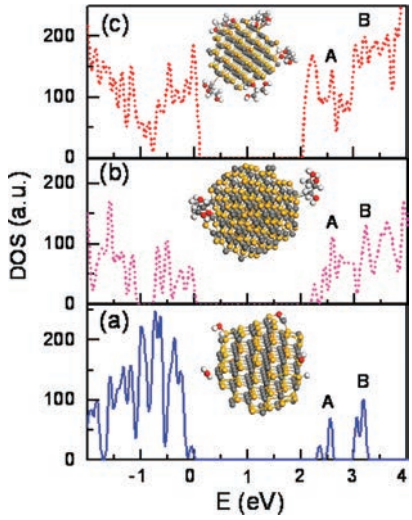

FIGURE 4. DOSs of 3C-SiC nanoclusters with different numbers of absorbed glycerol molecules. (a) 0, (b) 2, and (c) 5 molecules per NC. The insets show optimized structures of 3C-SiC nanoclusters with 5 water molecules in (a) and 2 and 5 glycerol molecules in (b) and (c) per NC. The yellow, gray, red, and white balls represent Si, C, O, and H atoms, respectively.

density of the added glycerol in the water suspension of 3C-SiC NCs is an important parameter to accomplish tunable emission. We have used a smaller amount of glycerol to passivate the NC surface but observed that the tunable PL intensity is significantly reduced. Hence, complete passivation of the NC surface is necessary in order to achieve strong tunable violet to blue-green emission.

To identify the effects of glycerol passivation and surface modification on the electronic structure, we conduct a density-functional-theory (DFT) study on the 3C-SiC NCs with and without absorbed glycerol molecules. The calculation is performed using the generalized gradient approximation of Perdew, Burke, and Ernzerholf[47] under package CASTEP[48] in which a norm-conserving pseudopotential method[49] is used. We use a kinetic energy cutoff of 470 eV for plane waves to represent the single-particle wave functions. We adopt a 3C-SiC nanocluster of diameter 1.6 nm with several glycerol molecules near its surface in a $2.5 \times 2.5 \times 2.5$ nm^3 supercell initially to perform geometry optimization and DFT band structure calculation. The other part of the supercell is vacuum and so the NCs are sufficiently separated.

The geometry of the nanoclusters together with adsorbed glycerol molecules is optimized using the BFGS minimizer in the CASTEP package with the following default convergence tolerances: energy of 2×10^{-5} eV, maximum force of 0.5 eV/nm, and maximum displacement of 0.02 nm.[50] The results pertaining to geometric optimization of 3C-SiC nanoclusters with 5 water molecules and 2 and 5 adsorbed glycerol molecules per NC are shown in the insets of Figures 4a−c, respectively. It can be seen that both the glycerol and water molecules are more likely to adsorb on the Si-terminated surface sections, while they are further apart from the C-terminated surface sections. Compared to the case involving water molecule adsorption,[34] adsorption of glycerol molecules causes more substantial surface modification, which may produce specific electronic structures.

Using the optimized structures, we calculate the energy band structure. The obtained densities of states (DOS) of the 3C-SiC nanoclusters with different number of adsorbed molecules are shown in Figure 4. It is known that the DFT calculation underestimates the energy gaps of SiC and their nanostructures.[12,15] In the case of zero-adsorbed molecule, there are two peaks marked as A and B in Figure 4a corresponding to the quantized levels of the conduction band due to the quantum size effect. Peak B can serve as the host states of the electrons excited from the valence band when excited by a laser, whereas peak A can accept electrons relaxing from B and provide PL when the electrons jump from A to the valence band. The energy position of peak A is almost fixed and so for NCs without attached glycerol molecule, it is difficult to tune the wavelength of the emitted photons by changing the frequency of the excitation laser. By gradually increasing the number of adsorbed glycerol molecules, both peaks A and B gradually transform to a continuum, as shown in Figure 4b,c. Consequently, by increasing the frequency of the excitation laser, the electrons can be pumped to higher levels in the upper quasi-continuous band and they will also relax to higher levels in the lower quasi-continuous band as the energy interval of the relaxation is almost unchanged if the relaxation mechanism is the same. Our experimental result in the inset of Figure 2b discloses that the relaxed energy interval is nearly constant. Therefore, glycerol absorption on 3C-SiC NCs further renders the possibility of tuning the wavelengths of the emitted photons by changing the frequency of the excitation laser. The tunable violet to blue-green emission observed in our experiments thus results from the mutual effects of size and glycerol bonding. From this point of view, other ligands that can effectively passivate the 3C-SiC surfaces without producing nonradiative defect states may also suffice.

As an application of the tunable solid film, we exploit the advance in broad emission from 3C-SiC NCs to fabricate full color solid film by combining with PS. Such a composite film structure is schematically plotted in Supposting Information Figure SI-2c. The glycerol coating renders the PS surface with good glycerol passivation and thus produces strong quantum-confined PL. In our experiments, the PL peak of the PS is strong and can be tuned from 580 to 760 nm when the excitation wavelength increases from 400 to 470 nm (the inset of Figure 5a). The PL spectra of the 3C-SiC NCs/PS solid film are shown in Figure 5a and they can be divided into three regions. In the violet-blue (360−500 nm) region, the tunable PL mainly originates from the quantum confinement effect of the 3C-SiC NCs. In the blue-red (500−620 nm) region, the visible emission stems from the contribution of both Si and 3C-SiC NCs. In the region between 620 and 780 nm, the PL mainly comes from the PS sample. Therefore, such a composite 3C-SiC NCs/PS solid film can emit strong

DOI: 10.1021/nl100407d | *Nano Lett.* **2010,** *10,* 1466–1471

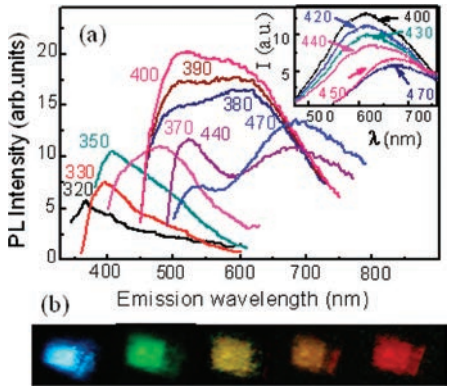

FIGURE 5. (a) PL spectra of the fabricated 3C-SiC NCs/PS solid film excited by different wavelengths. The inset shows the PL spectra of a PS sample excited by different wavelengths. (b) Light-emitting photos from the fabricated 3C-SiC NCs/PS solid film under excitation by five different wavelengths of 320, 400, 450, 470, and 500 nm. The emission wavelengths can be identified from left to right to be blue (~450 nm), green (~510 nm), yellow (~560 nm), orange (~600 nm), and red (~630 nm).

tunable PL in the entire visible region spanning 360 to 760 nm. Similar to the 3C-SiC/glycerol solid film, the full-color tunable PL is also very stable and no degradation is observed after storage in air for more than six months.

The PL of the 3C-SiC NCs/PS solid film is so intense that the emission spots with different wavelengths (colors) are visible to the naked eye even only by excitation of a Xe lamp. Figure 5b shows five typical emission photos taken using a Canon digital camera. Under the five different excitation wavelengths of 320, 400, 450, 470, and 500 nm, the emission spots appear to be blue (~450 nm), green (~510 nm), yellow (~560 nm), orange (~600 nm), and red (~630 nm), respectively. When taking these pictures, different filters are used to avoid scattering of the excitation light background. These color spots clearly demonstrate full-color tunable light emission from the solid composite nanostructured materials.

In conclusion, our experiments and calculation of the electron structures of the glycerol-passivated 3C-SiC NCs clearly show that glycerol can effectively passivate the complex surface/defect states of the 3C-SiC NCs. It produces a 3C-SiC NC solid film having strong (visible to the naked eyes) and tunable optical emission in violet to blue-green due to the surface modification on 3C-SiC NCs. The emission is very stable as demonstrated by that after the solid film has been stored in air for more than six months, no intensity degradation can be observed. Full-color (360−760 nm) tunable 3C-SiC/Si NC film can be made by embedding the glycerol-passivated 3C-SiC NCs on PS.

Acknowledgment. The authors sincerely thank Dr. S. D. Wang in the Nanomaterials and Soft Matter Laboratory, Suzhou University and Dr. W. S. Yan in the Synchrotron Radiation Laboratory, University of Science and Technology of China for performing the XPS and XANES measurements, respectively. This work was jointly supported by Grants (60876058, 10874071, 60976063, and BK2008020) from the National and Jiangsu Natural Science Foundations. Partial support was also from National Basic Research Programs of China under Grants 2007CB936301 and 2006CB921803 as well as Hong Kong Research Grants Council (RGC) General Research Grant (GRF) CityU 112307.

Supporting Information Available. XRD, molecular structure, and XANES spectra. This material is available free of charge via the Internet at http://pubs.acs.org.

REFERENCES AND NOTES

(1) Dai, H. J.; Wang, E. W.; Lu, Y. Z.; Fan, S. S.; Lieber, C. M. *Nature* **1995**, *375*, 769–772.
(2) Zhang, D. Q.; Alkhateeb, A.; Han, H. M.; Mahmood, H.; McIlroy, D. N.; Norton, M. G. *Nano Lett.* **2003**, *3*, 983–987.
(3) Xi, G. C.; Peng, Y. Y.; Pan, S. M.; Li, T. W.; Yu, W. C.; Qian, Y. T. *J. Phys. Chem. B* **2004**, *108*, 20102–20104.
(4) Wang, C. H.; Chang, Y. H.; Yen, M. Y.; Peng, C. W.; Lee, C. Y.; Chiu, H. T. *Adv. Mater.* **2005**, *17*, 419–422.
(5) Zhou, J.; Liu, J.; Yang, R. S.; Lao, C. S.; Gao, P. X.; Tummala, R.; Xu, N. S.; Wang, Z. L. *Small* **2006**, *2*, 1344–1347.
(6) Bechelany, M.; Brioude, A.; Stadelmann, P.; Ferro, G.; Cornu, D.; Miele, P. *Adv. Funct. Mater.* **2007**, *17*, 3251–3257.
(7) Wu, X. L.; Fan, J. Y.; Qiu, T.; Siu, G. G.; Chu, P. K. *Phys. Rev. Lett.* **2005**, *94*, No. 026102.
(8) Fan, J. Y.; Wu, X. L.; Li, H. X.; Liu, H. W.; Siu, G. G.; Chu, P. K. *Appl. Phys. Lett.* **2006**, *88*, No. 041909.
(9) Fan, J. Y.; Li, H. X.; Jiang, J.; So, L. K. Y.; Lan, Y. W.; Chu, P. K. *Small* **2008**, *4*, 1058–1062.
(10) Botsoa, J.; Lysenko, V.; Géloën, A.; Marty, O.; Bluet, J. M.; Guillot, G. *Appl. Phys. Lett.* **2008**, *92*, 173902.
(11) Fan, J. Y.; Wu, X. L.; Chu, P. K. *Prog. Mater. Sci.* **2006**, *51*, 983–1031.
(12) Cicero, G.; Catellani, A.; Galli, G. *Phys. Rev. Lett.* **2004**, *93*, No. 016102.
(13) Chang, H.; Wu, J.; Gu, B. L.; Liu, F.; Duan, W. H. *Phys. Rev. Lett.* **2005**, *95*, 196803.
(14) (a) Cicero, G.; Galli, G.; Catellani, A. *J. Phys. Chem. B* **2004**, *108*, 16518–16524. (b) Kanai, Y.; Cicero, G.; Selloni, A.; Car, R.; Galli, G. *J. Chem. Phys. B* **2005**, *109*, 13656–13662.
(15) Reboredo, F. A.; Pizzagalli, L.; Galli, G. *Nano Lett.* **2004**, *4*, 801–804.
(16) Peng, X. H.; Nayak, S. K.; Alizadeh, A.; Varanasi, K. K.; Bhate, N.; Rowland, L. B. *J. Appl. Phys.* **2007**, *102*, No. 024304.
(17) Derycke, V.; Soukiassian, P. G.; Amy, F.; Chabal, Y. J.; D'angelo, M. D.; Enriquez, H. B.; Silly, M. G. *Nat. Mater.* **2003**, *2*, 253–258.
(18) Wojtyk, J. T. C.; Tomietto, M.; Boukherroub, R.; Wayner, D. D. M. *J. Am. Chem. Soc.* **2001**, *123*, 1535–1536.
(19) Gillmor, S. D.; Thiel, A. J.; Strother, T. C.; Smith, L. M.; Lagally, M. G. *Langmuir* **2007**, *16*, 7223–72228.
(20) Buriak, J. M. *Chem. Rev.* **2002**, *102*, 1271–1308.
(21) Rosso, M.; Giesbers, M.; Arafat, A.; Schroen, K.; Zuilhof, H. *Langmuir* **2009**, *25*, 2172–2180.
(22) Rosso, M.; Arafat, A.; Schroen, K.; Giesbers, M.; Roper, C. S.; Maboudian, R.; Zuilhof, H. *Langmuir* **2008**, *24*, 4007–4012.
(23) Iijima, M.; Kamiya, H. *J. Phys. Chem. C* **2008**, *112*, 11786–11790.
(24) Niu, J. J.; Wang, J. N.; Xu, Q. F. *Langmuir* **2008**, *24*, 6918–6923.
(25) Zinovev, A. V.; Moore, J. F.; Hryn, J.; Pellin, M. J. *Surf. Sci.* **2006**, *600*, 2242–2251.
(26) Konstantinov, A. O.; Harris, C. I.; Janzen, E. *Appl. Phys. Lett.* **1994**, *65*, 2699–2701.
(27) Petrova-Koch, V.; Sreseli, O.; Polisski, G.; Kovalev, D.; Muschik, T.; Koch, F. *Thin Solid Films* **1995**, *255*, 107–110.
(28) Shor, J. S.; Bemis, L.; Kurtz, A. D.; Grimberg, I.; Weiss, B. Z.; Macmillian, M. F.; Choyke, W. J. *J. Appl. Phys.* **1994**, *76*, 4045–4049.
(29) Matsumoto, T.; Takahashi, J.; Tamaki, T.; Futagi, T.; Mimura, H.; Kanemitsu, Y. *Appl. Phys. Lett.* **1994**, *64*, 226–228.

DOI: 10.1021/nl100407d | *Nano Lett.* **2010,** *10,* 1466–1471

(30) Liao, L. S.; Bao, X. M.; Yang, Z. F.; Min, N. B. *Appl. Phys. Lett.* **1995**, *66*, 2382–2384.
(31) Rittenhouse, T. L.; Bohn, P. W.; Hossain, T. K.; Adesida, I.; Lindesay, J.; Marcus, A. *J. Appl. Phys.* **2003**, *95*, 490–496.
(32) Feng, D. H.; Xu, Z. Z.; Jia, T. Q.; Li, X. X.; Gong, S. Q. *Phys. Rev. B* **2003**, *66*, No. 035334.
(33) Kassiba, A.; Makowska-Janusik, M.; Bouclé, J.; Bardeau, J. F.; Bulou, A.; Herlin-Boime, N. *Phys. Rev. B* **2003**, *66*, No. 035334.
(34) Wu, X. L.; Xiong, S. J.; Zhu, J.; Wang, J.; Shen, J. C.; Chu, P. K. *Nano Lett.* **2009**, *9*, 4053–4060.
(35) Zhu, J.; Liu, Z.; Wu, X. L.; Xu, L. L.; Zhang, W. C.; Chu, P. K. *Nanotechnology* **2007**, *18*, 365603–365603.
(36) Wolfe, J. P. *Phys. Today* **1982**, *35*, 46–47.
(37) Reisfeld, R. *J. Alloys Compd.* **2002**, *341*, 56–61.
(38) Brus, L. *J. Phys. Chem.* **1986**, *90*, 2555–2560.
(39) Lee, K. H.; Lee, S. K.; Jeon, K. S. *Appl. Surf. Sci.* **2009**, *255*, 4414–4420.
(40) Bhattacharya, A. K.; Pyke, D. R.; Walker, G. S.; Werrett, C. R. *Appl. Surf. Sci.* **1997**, *108*, 465–470.
(41) Ohishi, K.; Hattori, T. *Jpn. J. Appl. Phys.* **1994**, *33*, L675–L678.
(42) Hollinger, G.; Himpsel, F. J. *Appl. Phys. Lett.* **1984**, *44*, 93–95.
(43) Verne, E.; Bretcanu, O.; Balagna, C.; Biabchi, C. L.; Cannas, M.; Gatti, S.; Vitale-Brovarone, C. *J. Mater. Sci: Mater. Med.* **2009**, *20*, 75–87.
(44) Jin, R. B.; Wu, Z. B.; Liu, Y.; Jiang, B. Q.; Wang, H. Q. *J. Hazard. Mater.* **2009**, *161*, 42–48.
(45) Holmes, J. D.; Ziegler, K. J.; Doty, R. C.; Pell, L. E.; Johnston, K. P.; Korgel, B. A. *J. Am. Chem. Soc.* **2001**, *123*, 3743–3748.
(46) Rosso-Vasic, M.; Spruijt, E.; van Lagen, B.; De Cola, L.; Zuilhof, H. *Small* **2008**, *4*, 1835–1841.
(47) Perdew, J. P.; Burke, K.; Ernzerhof, M. *Phys. Rev. Lett.* **1996**, *77*, 3865–3868.
(48) Clark, S. J.; Segall, M. D.; Pickard, C. J.; Hasnip, P. J.; Probert, M. J.; Refson, K.; Payne, M. C. *J. Crystallogr.* **2005**, *220*, 567–570.
(49) Hamann, D. R.; Schluter, M.; Chiang, C. *Phys. Rev. Lett.* **1979**, *43*, 1494–1497.
(50) Pfrommer, B. G.; Cote, M.; Louie, S. G.; Cohen, M. L. *J. Comput. Phys.* **1997**, *131*, 233–240.

DOI: 10.1021/nl100407d | *Nano Lett.* **2010,** *10,* 1466–-1471